

■ Carbene Complexes

Unusual NHC–Iridium(I) Complexes and Their Use in the Intramolecular Hydroamination of Unactivated Aminoalkenes**

Gellért Sipos,^[a] Arnold Ou,^[a] Brian W. Skelton,^[b] Laura Falivene,^[c] Luigi Cavallo,^{*,[c]} and Reto Dorta^{*,[a]}

Abstract: N-heterocyclic carbene (NHC) ligands with naphthyl side chains were employed for the synthesis of unsaturated, yet isolable [(NHC)Ir(cod)]⁺ (cod = 1,5-cyclooctadiene) complexes. These compounds are stabilised by an interaction of the aromatic wingtip that leads to a sideways tilt of the NHC–Ir bond. Detailed studies show how the tilting of such N-heterocyclic carbenes affects the electronic shielding

properties of the carbene carbon atom and how this is reflected by significant upfield shifts in the ¹³C NMR signals. When employed in the intramolecular hydroamination, these [(NHC)Ir(cod)]⁺ species show very high catalytic activity under mild reaction conditions. An enantiopure version of the catalyst system produces pyrrolidines with excellent enantioselectivities.

1. Introduction

Homogeneous catalysis based on metal complexes where bulky, monodentate ancillary ligands are used has gained enormous significance in the last two decades because it often provides catalytic systems with superior performance. For example, major developments in cross-coupling reactions have often relied on substituting multiple ligands or ligand chelates with a single, sterically demanding spectator ligand.^[1] Although the success of this approach is undeniable as it usually generates highly active and unsaturated metal complexes as catalytic species, rendering ligand systems overly bulky can lead to catalyst decomposition through unwanted activations of parts of the ligand that closely approach the metal centre.^[2]

Within the growing class of bulky, monodentate ancillary ligands, Arduengo-type N-heterocyclic carbenes (NHCs) have garnered increasing attention and have become ubiquitous ligands in transition-metal catalysis.^[3–5] Due to their strong σ -

donor ability and the high stability of their metal complexes they represent powerful tools in modern homogeneous catalyst development. Although dozens of monodentate NHCs have been synthesised to date, only a few of them have so far proven to be versatile as ancillary ligands. Data gathered so far would indicate that NHCs with perpendicularly oriented aromatic side chains offer a uniquely useful steric environment as exemplified by the very successful 1,3-bis(2,6-diisopropylphenyl)imidazol-2-ylidene/1,3-bis(2,6-diisopropylphenyl)-4,5-dihydroimidazol-2-ylidene (IPr/SIPr) and 1,3-bis(dimesityl)-imidazol-2-ylidene/1,3-bis(2,4,6-trimethylphenyl)-4,5-dihydroimidazol-2-ylidene (IMes/SIMes) ligand pairs.^[5]

In the past, we have identified NHCs with alkylated naphthyl wingtips as viable and often superior alternatives to these ligands.^[6] Incorporation of naphthalene units in NHC design had been reported before, and offers the option of a relatively straightforward introduction of a chiral element into the NHC ligand structure.^[7] In general, our ligands show increased reactivity also under forcing reaction conditions, which would point to a less ready deactivation of the catalyst through an unwanted metal–ligand reactivity. Even within this new class of NHCs, fine-tuning of the naphthyl side chain substituents of the ligands seems to be important. For example, when used as ligands in ruthenium metathesis, the particular substitution pattern of the side chains rendered the catalyst system more or less prone to decomposition through what appeared to be ruthenium-mediated cyclometalation reactions.^[6c] In another study on their application to NHC–Pd catalysts, the special steric bulk created by these ligands resulted in greatly improved reactivity in the Suzuki–Miyaura coupling reaction of sterically hindered aryls.^[6d]

Herein, we disclose studies that show how two representative members of our ligand systems (namely, ligands **1a** and **1b** in Scheme 1), although electronically very comparable to the classical IPr/SIPr and IMes/SIMes ligands, are able to stabi-

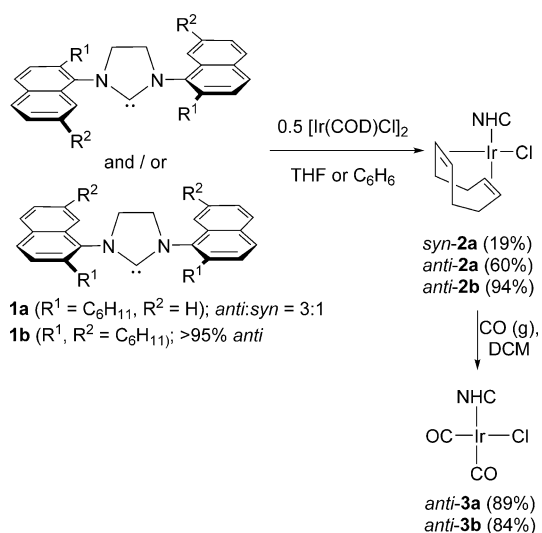
[a] G. Sipos, A. Ou, Prof. R. Dorta
School of Chemistry and Biochemistry
University of Western Australia
35 Stirling Highway
6009 Crawley, WA, (Australia)
E-mail: reto.dorta@uwa.edu.au

[b] Prof. B. W. Skelton
Centre for Microscopy, Characterisation and Analysis
University of Western Australia
35 Stirling Highway
6009 Crawley, WA, (Australia)

[c] Dr. L. Falivene, Prof. L. Cavallo
Kaust Catalysis Center, Physical Sciences and Engineering Division
King Abdullah University of Science and Technology
Thuwal 23955-6900 (Saudi Arabia)

[**] NHC = N-heterocyclic carbene.

Supporting information of this article can be found under <http://dx.doi.org/10.1002/chem.201600378>.



Scheme 1. Synthesis of neutral NHC–Ir^I complexes (cod = 1,5-cyclooctadiene).

lise formally three coordinate [NHC–Ir]⁺ systems through weak, non-destructive interactions of their side chains with the metal centre.^[8] We also show why and how the tilted nature of such NHC–M structures leads to significant upfield shifts in the ¹³C NMR signals. These unsaturated [NHC–Ir]⁺ species were then used in the intramolecular hydroamination (HA) of simple aminoalkenes,^[9] where developments within the last decade have established the usefulness of Group 9 metal complexes in the intramolecular HA of electronically unbiased aminoalkenes.^[10] Most notably, Hartwig et al. have developed cationic rhodium systems that contain phosphorous-based ancillary ligands,^[10b,g,i] whereas Stradiotto et al. have reported the use of simple [Ir(cod)Cl]₂ as the precatalyst.^[10c,e] These developments have broadened the scope of this simple and atom-economical reaction as they employ relatively easy-to-handle, functional-group-tolerant late-transition-metal catalysts for the construction of these important nitrogen heterocycles. Obviously, developing enantioselective versions of this transformation represents a particular challenge with any chiral ligand–metal com-

bination.^[10f,11] Although monodentate NHCs have previously been used in various iridium-catalysed transformations,^[8b,d,e,12] they have not been applied in the HA reaction of unactivated aminoalkenes.^[13] Here, we show how our special ligand architecture imparts unusually high reactivity and how we can extend the use of our ligands to the asymmetric version of this reaction, where systems based on iridium have been absent so far.^[14]

2. Results and Discussion

2.1. Synthesis and characterisation of the NHC–iridium complexes

Scheme 1 shows the synthetic pathway to neutral NHC–Ir systems employing two representatives of our NHC ligand family [i.e., 2-SiCyNap (1a) and 2,7-SiCyNap (1b)]. The [(NHC)Ir(cod)Cl] complexes **2a** and **2b** were obtained in good overall yields by reacting stoichiometric amounts of the free carbenes with 0.5 equivalents of [Ir(cod)Cl]₂ (Scheme 1).^[15] The *syn* and *anti* isomers of compound **2a** were separated by column chromatography.

The ¹H and the ¹³C NMR spectra of compounds *anti-2a* and *anti-2b* exhibit two distinct sets of signals for each of the naphthyl side chains (i.e., twenty carbon signals can be observed). The two methylene carbon atoms of the imidazolidine backbone are clearly distinguishable in these complexes ($\delta = 54.8$ and 54.4 ppm for *anti-2a*; $\delta = 54.5$ and 54.0 ppm for *anti-2b*). Also, the CH=CH fragments of the cod ligand are represented by four distinct sets of signals both in the ¹H and ¹³C NMR spectra. Finally, the most characteristic resonance (of the NHC) in the ¹³C NMR spectra is found at around $\delta = 210$ ppm.

The synthesis and full characterisation of complexes **2** (the molecular structures of which are shown in Figure 1) set the stage to evaluate the electronic properties of our NHC ligands **1a** and **1b**. The carbonyl complexes were accessed in high yield by reacting compounds *anti-2a* and *anti-2b* with carbon monoxide.^[16] Somewhat expectedly, complexes *anti-3a* and *anti-3b* showed Tolman electronic parameter (TEP) values very

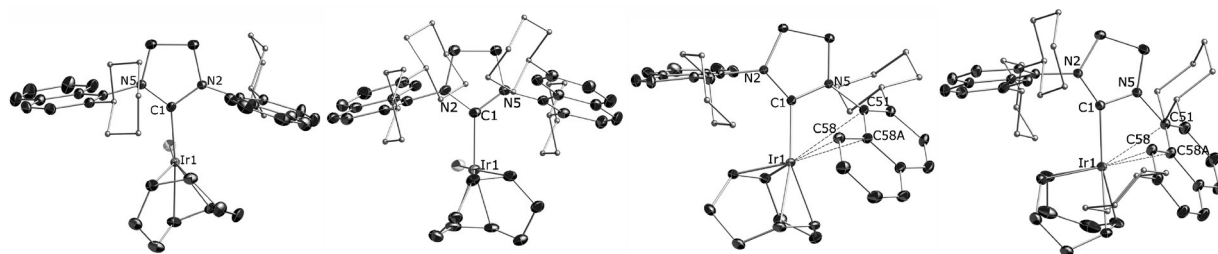


Figure 1. Molecular structures of compounds (from left to right) *anti-2a*, *anti-2b*, *anti-4a* and *anti-4b*. For cationic complexes, the anion is omitted for clarity. All hydrogen atoms are omitted for clarity and the cyclohexyl groups are represented differently for the same reason. Selected bond lengths [Å] and angles [°]: for compound *anti-2a*: Ir–C1 2.034(1), Ir–C11 2.147(1), Ir–C12 2.147(1), Ir–C15 2.127(1), Ir–C16 2.094(1), Ir–Cl 2.3645(3); Ir–C1–N2 120.70(9), Ir–C1–N5 131.31(9); for compound *anti-2b*: Ir–C1 2.052(5), Ir–C11 2.194(5), Ir–C12 2.173(6), Ir–C15 2.121(5), Ir–C16 2.113(6), Ir–Cl 2.350(1); Ir–C1–N2 126.0(4), Ir–C1–N5 127.2(4); for compound *anti-4a*: Ir–C1 2.041(1), Ir–C11 2.178(1), Ir–C12 2.233(1), Ir–C15 2.101(1), Ir–C16 2.104(1), Ir–C51 2.981(1), Ir–C58 2.407(1), Ir–C58A 2.666(1); Ir–C1–N2 134.56(9), Ir–C1–N5 116.00(8); for compound *anti-4b*: Ir–C1 2.038(2), Ir–C11 2.181(2), Ir–C12 2.224(2), Ir–C15 2.091(2), Ir–C16 2.114(2), Ir–C51 2.591(1), Ir–C58 2.544(2), Ir–C58A 2.413(2); Ir–C1–N2 145.0(1), Ir–C1–N5 106.7(1).

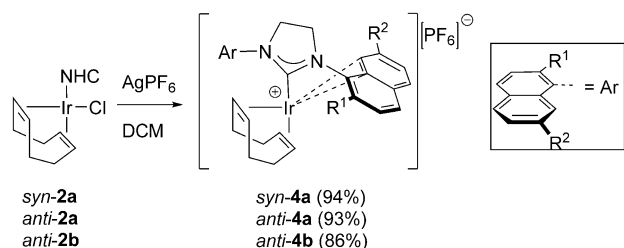
similar to the established SIMes/IMes and SIPr/IPr ligand pairs (Table 1).^[8c, 15, 17] However, we note that the second cyclohexyl substituent (position 7) is rendering ligand **1b** more electron-donating, much in the same way as seen when going from the saturated to the unsaturated NHC analogues of the standard ligands SIMes/IMes and SIPr/IPr.

Table 1. Carbonyl stretching frequencies for the complexes [(NHC)Ir(CO)₂Cl] and [(NHC)Ni(CO)₃].

NHC	$\tilde{\nu}_{\text{CO}}$ [cm ⁻¹]	$\tilde{\nu}_{\text{CO}}^{\text{av}}$ [cm ⁻¹]	TEP [cm ⁻¹]
2-SiCyNap (1a)	2067.4, 1982.7	2025.0	2051.2 ^[a]
2,7-SiCyNap (1b)	2066.5, 1981.3	2023.9	2050.3 ^[a]
SIPr ^[b]	2068.0, 1981.8	2024.9	2051.2
IPr ^[b]	2066.8, 1981.0	2023.9	2050.2
SIMes ^[b]	2068.0, 1981.2	2024.6	2050.8
IMes ^[b]	2066.4, 1979.8	2023.1	2049.6

[a] Calculated with the formula: $\text{TEP} = 0.847 \times \tilde{\nu}^{\text{av}} + 336$ [cm⁻¹]. [b] Taken from reference [17b].

The [(NHC)Ir(cod)Cl] complexes *syn-2a*, *anti-2a* and *anti-2b* also gave us a very interesting entry into ligand degradation problems mentioned in the introduction. In a recent paper, Aldridge et al. had studied the outcome of the reaction of [(IPr)Ir(cod)Cl] with Na(BAr^f₄)^[18, 19c] where abstraction of the chloride led to a highly reactive metal species that underwent ready C–H activation and dehydrogenation of one of the isopropyl moieties of the wingtips. In stark contrast, halide abstraction on compounds *syn-2a*, *anti-2a* and *anti-2b* gave deep red, crystalline materials where X-ray diffraction analyses of compounds *syn-4a*, *anti-4a* and *anti-4b* confirmed the composition of the complexes as being [(NHC)Ir(cod)](PF₆) (Scheme 2).^[20] Representations of compounds *anti-4a* and *anti-4b* (Figure 1) reveal that cyclometalation does not occur and in order to stabilise these formally 14-electron species,^[21] one of the aromatic wingtips approaches the metal centre and displays an arene–metal interaction that involves the C8 and C8a carbon atoms of the naphthyl unit (C58 and C58a in the crystallographic numbering; the Ir–C bond lengths are 2.407(1)/2.666(1) Å for compound *anti-4a* and 2.544(2)/2.413(2) Å for compound *anti-4b*) and leads to a pseudo-square-planar coordination geometry.^[22] As a consequence, the NHC ring is tilted towards the side where the interaction occurs.^[23] This affords disparate Ir–C1–N2 and Ir–C1–N5 angles (namely, 134.56(8)/116.00(8)° for compound *anti-4a* and 145.0(1)/106.7(1)° for



Scheme 2. Synthesis of cationic NHC–Ir^I complexes.

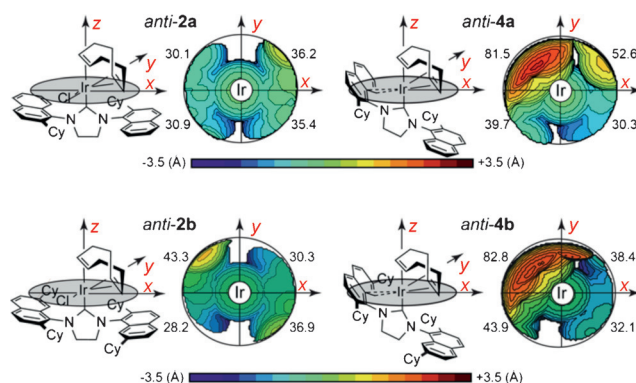


Figure 2. Steric maps of the neutral complexes *anti-2a* and *anti-2b* and the cationic complexes *anti-4a* and *anti-4b*. Isocontour lines are given in [Å].

compound *anti-4b*) and also impacts space occupation around the metal centre. As evidenced by the steric quadrant maps shown in Figure 2, the tilting results in a %V_{Bur} (percent buried volume) of approximately 80% of the relevant quadrant and leads to a significant increase in overall ligand bulk.

NMR spectroscopy indicated that the arene interaction might not be present in solution. The proton spectra of compounds *anti-4a* and *anti-4b* were highly simplified compared to the parent neutral complexes and the two naphthyl rings appeared to be identical on the ¹H NMR time scale. Nevertheless, the ¹H NMR analysis of the *syn-4a* isomer at 298 K showed very broad signals, and a variable-temperature (VT) analysis of compound *anti-4b*, although inconclusive, indicated that both the COD and the NHC ligand undergo fluxional processes. More insightful information was gathered through analyses of the ¹³C NMR spectra. The signals for the C8 and C8a carbon atoms of the two naphthyl rings showed broad singlets significantly upfield with respect to their neutral counterparts ($\delta(\text{C8}) = 107.2/\delta(\text{C8a}) = 126.0$ ppm for *anti-4a*; $\delta(\text{C8}) = 107.0/\delta(\text{C8a}) = 123.6$ for *anti-4b*), which would be expected when binding interactions with the metal are present. Unusually large shifts were also measured for the carbene carbon atoms, whose signals are positioned approximately 20 ppm upfield from their neutral congeners ($\delta = 196.0$ ppm for *anti-4a* and $\delta = 188.1$ ppm for *anti-4b*). At first sight, we attributed these large shifts to the tilt of the N-heterocycle that is maintained in solution and influences the electronic environment of the carbene carbon atom. Evidence for such a scenario came from an experiment whereby compound *anti-4b* was dissolved in CD₃CN. A new, dissymmetric species (namely, [(*anti-1b*)Ir(cod)(CD₃CN)](PF₆)) was formed with NMR data mirroring the ones seen for *anti-2b* and where the carbene carbon atom was found at $\delta = 200.5$ ppm.^[24]

2.2. Computational analysis of tilted NHC–M compounds

To shed light on the origin of the upfield shift of the carbene carbon atom NMR signals in our tilted structures, we performed DFT NMR calculations.^[16, 25] We initially tested the computational setup to reproduce the crystallographic geometry and the experimental chemical shift, δ_{C} of twelve monoden-

tate and chelating NHC–M complexes described in the literature^[23b,26] (see Figure S11 in the Supporting Information) plus the free NHC ligand **1b** and the corresponding protonated form, **1b**·H⁺. We selected these compounds because they represent pairs of related complexes presenting linear and bent NHC–M bonds, for which the crystallographic structure and ¹³C NMR data are available.

To check for the validity of the chosen computational approach in reproducing the geometry of the complexes examined, we compared the main structural parameters from the DFT optimisation, which is the M–NHC bond length and the M–C–N(NHC) angles, with the values of the crystallographic structure (see Table S2 in the Supporting Information). The excellent agreement between the DFT-optimised and the crystallographic parameters, with mean unsigned error on the M–NHC bond length of only 0.013 Å, and on the M–C–N1 and M–C–N2 angles of 0.81 and 1.04°, respectively, validate the methodology we used to calculate the geometries of this series of M–NHC complexes. To check for the validity of the chosen DFT NMR protocol, we tested it to reproduce the experimental δ_C values of the examined complexes. The excellent correlation ($R^2=0.93$) between the DFT isotropic chemical shielding σ_C values and the experimental δ_C values of the carbene carbon atoms (see Figure S12 in the Supporting Information) validates the DFT NMR part of the computational setup.

At this point, we moved to decipher the origin of the upfield shift due to the bending of the M–NHC bond. To this end, we used the model system NHC–Se shown in Figure 3, because it

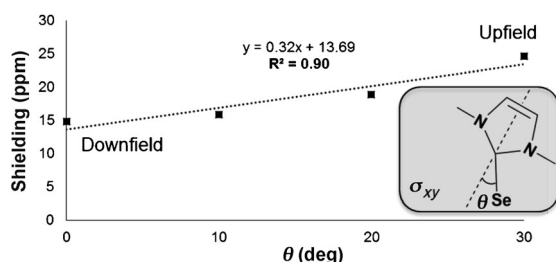


Figure 3. DFT-calculated chemical shielding versus the tilt angle for the NHC–Se bond.

was demonstrated that the NHC–Se bond is a good mimic of the NHC–M bond.^[25,27] Starting from a linear geometry, we tilted the NHC–Se bond by $\theta=10, 20$ and 30° . For each structure we calculated the σ_C value of the carbene atom. Gratifyingly, also the σ_C values of the NHC–Se system moves upfield as the NHC–Se bond is tilted (Figure 3), and the shift, approximately 10 ppm, is consistent with the experimental shift in the NHC–M complexes we investigated. The strong correlation ($R^2=0.90$) between the σ_C value and θ indicates that the upfield shift is essentially due to the tilting.

Decomposing the isotropic chemical shielding σ_C into diamagnetic (σ_d) and paramagnetic (σ_p) terms, $\sigma_C = \sigma_d + \sigma_p$, indicates that the change in σ_C is due to the paramagnetic term σ_p that varies by 6.5 ppm from 0 to 30° , whereas the diamagnetic term σ_d varies by only 0.1 ppm. The paramagnetic shielding depends from

transition of electrons between occupied and virtual orbitals, properly connected by symmetry, induced by the external magnetic field (e.g., $p_x \rightarrow p_z$ by 90° rotation around the y axis). The amount of the shielding is inversely related to the energy gap between these two orbitals, and it is directly related to a proper overlap of the orbitals after rotation.^[28] Correlation of the paramagnetic term to the molecular properties thus should focus on these two factors, which affect the paramagnetic shielding.

Because the σ_p term is dominated by transitions between symmetry-related occupied and empty molecular orbitals (MOs)^[28] based on previous work,^[27a] we focused on changes in energy and shape of the filled and empty MOs corresponding to the σ and π^* orbitals of the Se–NHC bond at $\theta=0$ and 30° .^[16,28] Whereas the connection between the paramagnetic shielding and the energy gap between these MOs is quite simple, the smaller the gap the larger the shielding, the required symmetry relation between the MOs is explained in Figure 4a. In the linear geometry, rotation of the MO induced by an external magnetic field results in MOs having the same symmetry and an optimal overlap, because the σ -bonding MO is mainly composed by p_x atomic orbitals (AOs) on both the carbenic carbon atom and the Se atom (see Figures 4a and b).

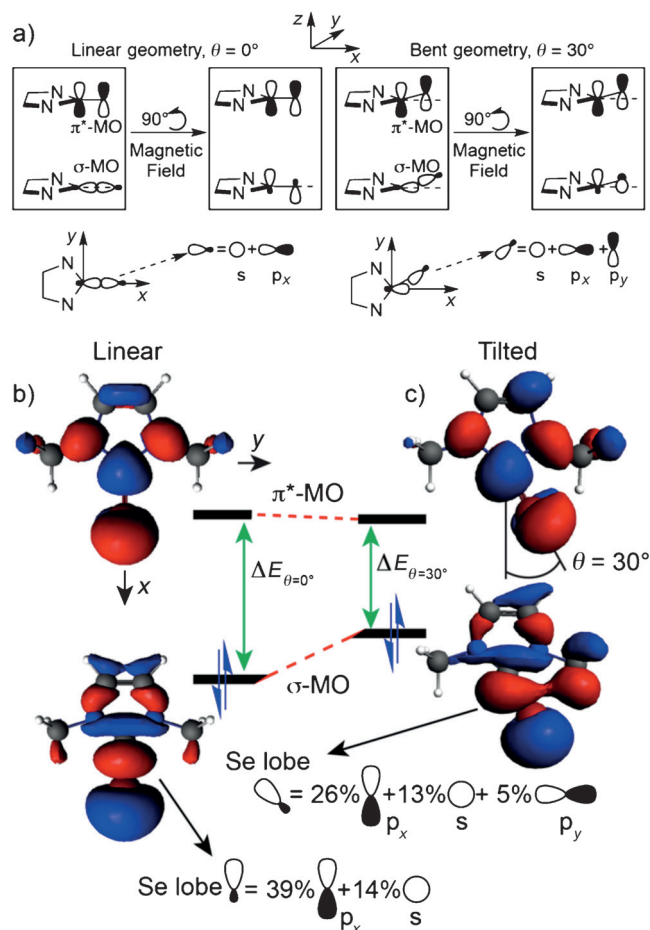


Figure 4. a) Schematic representation of the magnetic $\sigma \rightarrow \pi^*$ coupling. b, c) Analysis of the MOs corresponding to the σ and π^* Se–NHC bonds.

This optimal overlap results in a strong magnetic coupling between the σ and π^* MOs, with strong paramagnetic deshielding of the carbenic carbon atom. Differently, in the bent geometry the same rotation results in a non-optimal overlap of the MOs, due to the different composition of the σ -bonding MO on Se (see Figures 4a and c). Due to the tilting, hybridisation of the Se atoms moves from a dominant participation of the p_x AO to a mixture of p_x and p_y AOs, in order to orient the σ -bonding lobe on the Se towards the NHC (see Figure 4c). The p_x component of the bonding lobe on the Se is still capable of magnetic coupling with the π^* MO by 90° rotation, whereas the p_y component has not the proper symmetry, and thus does not contribute to the paramagnetic shielding. The reduced amount of the p_x component in the NHC–Se σ bond on going from a linear to a bent geometry results in weaker magnetic coupling between the σ and π^* MOs in the bent geometry and, consequently, in smaller paramagnetic deshielding and upfield shift of the carbenic resonance. Extension of these concepts to a NHC–M complex is straightforward.

Quantitatively, our analysis indicates that a bending of 30° of the NHC–Se bond destabilises the M–NHC σ -bonding MO by 0.54 eV, whereas the NHC–Se π^* MO is stabilised by 0.24 eV, with a decrease of 0.78 eV of the energy gap between them (Figure S13 in the Supporting Information). The representation of these MOs at $\theta=0$ and 30° (Figure 4) suggests that destabilisation of the NHC–Se σ -bonding MO is due to a misalignment of the in phase lobes on the NHC and the Se atom. Differently, the NHC–Se π^* MO is less affected because the tilting does not reduce the overlap of the p_z orbitals on the carbene carbon and Se atoms. The reduced energy gap between the σ and π^* MOs should shift the carbene atom downfield. However, the weight of the p_x atomic orbital on the Se atom in the NHC–Se σ -bonding MO, which is the atomic orbital having a proper symmetry relation for overlap with the NHC–Se π^* MOs after 90° rotation, is strongly reduced with tilting (from 39 to 26%, see Figure 4). This translates into poorer magnetic coupling and causes the observed upfield shift of the carbene atom.^[16]

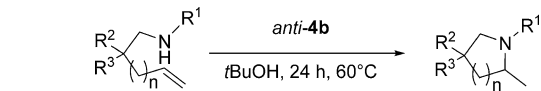
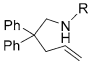
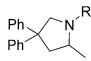
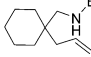
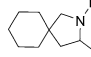
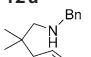
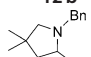
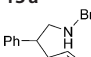
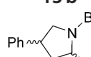
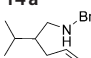
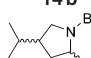
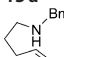
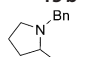
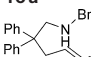
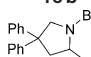
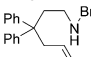
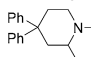
2.3. Catalytic application in the intramolecular hydroamination reaction

The catalytic behaviour of complexes **4** was then explored in the intramolecular HA reaction. In a first stage, we tested the cationic complexes *syn-4a*, *anti-4a* and *anti-4b* with the model substrate **5a** and monitored their performance by using ^1H NMR spectroscopy (Figure S8 in the Supporting Information). Cyclisation occurred with a catalyst loading of 0.5 mol% at room temperature and an especially impressive performance was achieved with compound *anti-4b*, with full conversion attained within approximately 3.5 min (turnover frequency (TOF) of $\approx 3500\text{ h}^{-1}$). Generating the complex *anti-4b* in situ by mixing equimolar amounts of *anti-2b* and AgPF_6 in dichloromethane prior to adding substrate **5a** replicated the results seen for the preformed catalyst *anti-4b*. In stark contrast, by using the similarly bulky and electronically analogous SIPr ligand (i.e., $[(\text{SIPr})\text{Ir}(\text{cod})\text{Cl}]+\text{AgPF}_6$) led to a totally inefficient

catalyst even when increasing the catalyst loading tenfold (i.e., to 5 mol%).

Subsequently, a variety of substrates were tested with catalyst *anti-4b* and the obtained results are summarised in Table 2. For these reactions, we chose *t*BuOH as the solvent because not only did it show comparable reactivity with model substrate **5a**, but reactions with other substrates gave less secondary products that arise from isomerisation of the olefin moiety. Examples of successfully ring-closed substrates include a variety of electron-donating and -withdrawing benzyl groups which are tolerated and lead to high yields of product at low catalyst loadings of *anti-4b* (products **6–8** in Table 2). Substrates with aliphatic groups on the nitrogen atom went through the cyclisation smoothly (products **9** and **10** in Table 2). Hydroamination of aryl amine (**11a**), which was described as a limitation for cationic rhodium systems,^[10g] gave the corresponding pyrrolidine (**11b**) in good yield.

Table 2. Scope of the intramolecular HA reaction catalysed by compound *anti-4b*.

			
Substrate	Product	Ir [mol%] ^[a]	Yield [%] ^[b]
			
5a R = CH ₂ (C ₆ H ₅) (Bn)	5b	0.25	96
6a R = CH ₂ (4-MeOC ₆ H ₄)	6b	1.5	93
7a R = CH ₂ (4-ClC ₆ H ₄)	7b	0.5	91
8a R = CH ₂ (4-NO ₂ C ₆ H ₄)	8b	2	79
9a R = CH ₂ (C ₆ H ₁₁)	9b	0.5	95
10a R = Me	10b	0.25	93
11a R = C ₆ H ₅	11b	1.0	96
			
12a	12b	0.5	88
			
13a	13b	1.0	86 (> 99) ^[c]
			
14a	14b	1.5	95 (3:2) ^[d]
			
15a	15b	1.0	96 (3:2) ^[d]
			
16a	16b	3.5	82 ^[c]
			
17a	17b	5	traces
			
18a	18b	5	77 ^[c]

[a] General conditions: 0.3 mmol substrate, compound *anti-4b*, 0.5 mL *t*BuOH, 60°C , 24 h. [b] Yields of isolated compounds. [c] ^1H NMR yield by using internal standard. [d] Diastereomeric ratio determined by ^1H NMR spectroscopy.

The backbone of the substrate can be modified to include a variety of substituents (compare **5** and **12–16** in Table 2) and although the Thorpe–Ingold effect clearly helps cyclisation, substrate **16a** that lacks backbone substitution underwent cyclisation smoothly with higher catalyst loadings (3.5 mol%). This is in contrast to the simple $[\text{Ir}(\text{cod})\text{Cl}]_2$ system described by Stradiotto et al.,^[10e] which is not able to cyclise this type of substrates. A higher catalyst loading of *anti*-**4b** was also needed for the formation of the six-membered piperidine **18b**. Some limitations remain however under our chosen reaction conditions. For example, the cyclisation of the internal alkene **17a** only led to trace amounts of the expected product **17b**, and what *anti*-**4b** shares with $[\text{Ir}(\text{cod})\text{Cl}]_2$ is the inability to cyclise primary amines under these conditions (i.e., no additives). Overall though, the results listed in Table 2 show that surprisingly low catalyst loadings and mild reaction conditions can be used in the intramolecular HA with catalyst *anti*-**4b**.

2.4. Asymmetric intramolecular hydroamination reaction

An intriguingly simple possibility to further extend the utility of our catalyst system arose from the fact that the NHCs used above can rather easily be modified to produce enantiopure ligand frameworks, as previously described by us.^[29] To this aim and to keep the overall catalytic system as similar as possible to *anti*-**4a** respectively *anti*-**4b**, we used a close relative of ligand **1a** that we had previously used in a palladium-catalysed asymmetric α -arylation protocol.^[29a] The corresponding cationic complex ($R_{ar}R_{ar}S,S$)-**19** (Table 3) was isolated in 52% overall yield (over two steps) from the corresponding NHC salt. The reactivity of compound **19** (for reasons unknown at present) was significantly lower when compared to its immediate counterpart *anti*-**4a** when monitoring the conversion of substrate **5a**. Furthermore and in contrast to *anti*-**4b**, catalyst **19** did not react smoothly with substrates in *t*BuOH. Nevertheless, reactions run in dichloromethane showed that ready cyclisation occurs under mild conditions when raising the catalyst loading. The enantioselectivities that we recorded with the substrates chosen for this brief survey are excellent and indeed, the enantiomeric excess (*ee*) values obtained for these pyrrolidines are amongst the highest reported for the asymmetric intramolecular HA of unactivated aminoolefins.^[30] Furthermore, the fact that the present system seems to be rather insensitive to the nature of the nitrogen substitution (benzyl or alkyl), bodes well for further development of this new chiral catalyst platform.^[31]

2.5. Possible deactivation pathway of the $[(\text{NHC})\text{Ir}(\text{cod})][\text{PF}_6]$ catalysts in dichloromethane

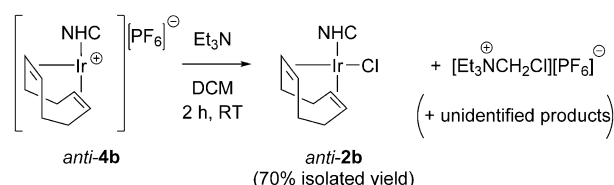
As outlined above, we did see some differences in the behaviour of both catalysts *anti*-**4b** and enantiopure ($R_{ar}R_{ar}S,S$)-**19** in terms of suitability of the solvent, with *anti*-**4b** performing better in *t*BuOH than dichloromethane, especially for the less reactive substrates. Although a more thorough investigation is needed to fully understand how the solvent influences the outcome of these HA reactions, a preliminary result that we

Table 3. Asymmetric intramolecular HA reaction catalysed by compound ($R_{ar}R_{ar}S,S$)-**19**.^[a]

<p>5b^[b] 90% yield 98% <i>ee</i></p>	<p>7b 94% yield 94% <i>ee</i></p>	
<p>9b 81% yield 95% <i>ee</i></p>	<p>10b 95% yield 87% <i>ee</i></p>	<p>13b 69% yield 95% <i>ee</i></p>

[a] General conditions: 0.3 mmol substrate, **19** (5 mol%), CH_2Cl_2 (0.5 mL), 7 °C, 24 h. Yields of isolated compounds. The *ee* was determined by ^1H NMR spectroscopy. [b] **19** (2 mol%) was used, the *ee* was determined by HPLC.

were able to gather with *anti*-**4b** in dichloromethane in the presence of a stoichiometric amount of triethylamine is relevant and noteworthy. Scheme 3 shows that *anti*-**4b** rapidly decomposes in the presence of this simple tertiary amine in dichloromethane to give good isolated yields of the starting chloride complex *anti*-**2b**, which is not catalytically active in



Scheme 3. Reactivity of Et_3N with dichloromethane accelerated by complex *anti*-**4b**.

the intramolecular HA reaction described here. It is known that triethylamine (and other amines) can be alkylated by methylene chloride (Menshutkin reaction),^[32] but the reaction is normally negligible due to its very slow reaction rate (half-life over a month for triethylamine).^[33] The reactivity in Scheme 3 shows that *anti*-**4b** is able to greatly accelerate this transformation.^[34] Although more detailed information will have to be gathered in the future with regards to similar reactivity with amines that are substrates and/or products of the intramolecular HA protocol, it seems likely that this decomposition pathway is operative to some degree in the overall catalytic transformation described here.

3. Conclusion

In conclusion, we have synthesised unusual $[(\text{NHC})\text{Ir}(\text{cod})][\text{PF}_6]$ complexes where an additional binding interaction is present. The interaction stabilises an otherwise very reactive 14-electron Ir^I species and at the same time significantly increases the steric bulk of the ligand, as quantified by steric quadrant maps. The interaction also leads to a sideways tilt of the NHC–M bond that translates into a large upfield shift of the carbene carbon NMR signal. DFT calculations have allowed us to show that this is a general phenomenon of such tilted NHCs. It can be attributed to the paramagnetic component of the isotropic shielding and is due to the misalignment of the bonding lobes forming the NHC–M σ bond. The non-destructive nature of the wingtip interaction is at the heart of the excellent performance of the complexes when employed as catalysts in the intramolecular HA reaction. Notably, first results employing an enantiopure version of our NHC gave a catalyst that provided excellent enantioselectivities in the asymmetric version of this HA. Because the catalytic results here are a first for the monodentate NHC ligand class, further investigations will be needed to understand how steric and electronic tuning of the NHC moiety affects the catalytic performance. A major goal of these studies will be to conjure up chiral catalyst systems that show similarly high reactivity to complex **anti-4b**. Detailed mechanistic studies will also be conducted to shed light onto the catalytic reaction cycle and will have to take into account our preliminary, intriguing data on solvent participation to catalyst decomposition.

Acknowledgements

G.S. thanks the UWA for an International Postgraduate Research Scholarship. R.D. thanks the Australian Research Council for generous funding (FT130101713). The Centre for Microscopy, Characterisation & Analysis at the UWA is thanked for providing facilities and assistance. L.C. thanks the King Abdullah University of Science and Technology for financial support.

Keywords: carbenes • density functional calculations • hydroamination • heterocycles • iridium

- [1] For books and reviews, see: a) *New Trends in Cross-Coupling: Theory and Applications* (Ed.: T. Colacot), RSC, Cambridge, **2015**; b) P. G. Gildner, T. J. Colacot, *Organometallics* **2015**, *34*, 5497; c) F. Izquierdo, S. Manzini, S. P. Nolan, *Chem. Commun.* **2014**, *50*, 14926; d) C. Valente, S. Çalimsiz, K. H. Hoi, D. Mallik, M. Sayah, M. G. Organ, *Angew. Chem. Int. Ed.* **2012**, *51*, 3314; *Angew. Chem.* **2012**, *124*, 3370. For selected recent examples, see: e) N. H. Park, E. V. Vinogradova, D. S. Surry, S. L. Buchwald, *Angew. Chem. Int. Ed.* **2015**, *54*, 8259; *Angew. Chem.* **2015**, *127*, 8377; f) S. Sharif, R. P. Rucker, N. Chandrasoma, D. Mitchell, M. J. Rodriguez, R. D. J. Froese, M. G. Organ, *Angew. Chem. Int. Ed.* **2015**, *54*, 9507; *Angew. Chem.* **2015**, *127*, 9643; g) D. Maiti, B. P. Fors, J. L. Henderson, Y. Nakamura, S. L. Buchwald, *Chem. Sci.* **2011**, *2*, 57.
- [2] For an excellent recent review on the topic of catalyst decomposition, see: R. H. Crabtree, *Chem. Rev.* **2015**, *115*, 127.
- [3] For books on the subject, see: a) *N-Heterocyclic Carbenes in Synthesis* (Ed.: S. P. Nolan), Wiley-VCH, Weinheim, **2006**; b) *N-Heterocyclic Carbenes in Transition-Metal Catalysis* (Eds.: F. Glorius, S. Bellemin-Lapponnaz), Springer, Heidelberg, **2007**; c) *N-Heterocyclic Carbenes in Transition-Metal Catalysis and Organocatalysis* (Ed.: C. S. J. Cazin), Springer, Heidelberg, **2010**; d) *N-Heterocyclic Carbenes: From Laboratory Curiosities to Efficient Synthetic Tools* (Ed.: S. Díez-González), RSC, Cambridge, **2011**; e) *N-Heterocyclic Carbenes* (Ed.: S. P. Nolan), Wiley-VCH, Weinheim, **2014**. For a short account, see: f) M. N. Hopkinson, C. Richter, M. Schedler, F. Glorius, *Nature* **2014**, *510*, 485.
- [4] For selected reviews on the subject, see: a) S. Díez-González, N. Marion, S. P. Nolan, *Chem. Rev.* **2009**, *109*, 3612; b) G. C. Vougioukalakis, R. H. Grubbs, *Chem. Rev.* **2010**, *110*, 1746; c) F. Wang, L. J. Liu, W. Wang, S. Li, M. Shi, *Coord. Chem. Rev.* **2012**, *256*, 804. For NHC synthesis, see: d) P. de Frémont, N. Marion, S. P. Nolan, *Coord. Chem. Rev.* **2009**, *253*, 862; e) L. Benhamou, E. Chardon, G. Lavigne, S. Bellemin-Lapponnaz, V. César, *Chem. Rev.* **2011**, *111*, 2705. For NHC stability and reactivity, see: f) C. M. Crudden, D. P. Allen, *Coord. Chem. Rev.* **2004**, *248*, 2247. For M–NHC bonds, see: g) H. Jacobsen, A. Correa, A. Poater, C. Costabile, L. Cavallo, *Coord. Chem. Rev.* **2009**, *253*, 687.
- [5] For first reports on their synthesis and characterisation, see: a) A. J. Arduengo, H. V. R. Dias, R. L. Harlow, M. Kline, *J. Am. Chem. Soc.* **1992**, *114*, 5530; b) A. J. Arduengo, J. R. Goerlich, W. J. Marshall, *J. Am. Chem. Soc.* **1995**, *117*, 11027; c) A. J. Arduengo, R. Krafczyk, R. Schmutzler, H. A. Craig, J. R. Goerlich, W. J. Marshall, M. Unverzagt, *Tetrahedron* **1999**, *55*, 14523.
- [6] For selected examples from our laboratory, see: a) X. Luan, R. Mariz, M. Gatti, C. Costabile, A. Poater, L. Cavallo, A. Linden, R. Dorta, *J. Am. Chem. Soc.* **2008**, *130*, 6848; b) L. Vieille-Petit, X. Luan, R. Mariz, S. Blumentritt, A. Linden, R. Dorta, *Eur. J. Inorg. Chem.* **2009**, 1861; c) L. Vieille-Petit, X. Luan, M. Gatti, S. Blumentritt, A. Linden, H. Clavier, S. P. Nolan, R. Dorta, *Chem. Commun.* **2009**, 3783; d) L. Wu, E. Drinkel, F. Gaggia, S. Capolicchio, A. Linden, L. Falivene, L. Cavallo, R. Dorta, *Chem. Eur. J.* **2011**, *17*, 12886; e) M. Gatti, L. Wu, E. Drinkel, F. Gaggia, S. Blumentritt, A. Linden, R. Dorta, *ARKIVOC* **2011**, 6, 176.
- [7] For selected examples where naphthalene units are used in the design of NHC ligands, see: a) W. A. Herrmann, L. J. Goossen, C. Köcher, G. R. J. Artus, *Angew. Chem. Int. Ed. Engl.* **1996**, *35*, 2805; *Angew. Chem.* **1996**, *108*, 2980; b) D. S. Clyne, J. Jin, E. Genest, J. C. Gallucci, T. V. RajanBabu, *Org. Lett.* **2000**, *2*, 1125; c) J. J. van Veldhuizen, S. B. Garber, J. S. Kingsbury, A. H. Hoveyda, *J. Am. Chem. Soc.* **2002**, *124*, 4954; d) E. Bappert, G. Helmchen, *Synlett* **2004**, 1789; e) O. Winkelmann, D. Linder, J. Lacour, C. Näther, U. Lüning, *Eur. J. Org. Chem.* **2007**, 3687; f) M. Nakanishi, D. Katsayev, C. Besnard, E. P. Kündig, *Angew. Chem. Int. Ed.* **2011**, *50*, 7438; *Angew. Chem.* **2011**, *123*, 7576.
- [8] Examples of neutral $[(\text{NHC})\text{Ir}(\text{cod})\text{X}]$ (X = anionic ligand) and $[(\text{NHC})\text{Ir}(\text{cod})\text{L}]^+$ (L = neutral two-electron donor) complexes are abundant in the literature. For overviews, see examples reviewed in references [3] and [4], as well as a) *Iridium Complexes in Organic Synthesis* (Eds.: L. A. Oro, C. Claver), Wiley-VCH, Weinheim, **2009**, Chapter 3. For some selected examples, see: b) H. M. Lee, T. Jiang, E. D. Stevens, S. P. Nolan, *Organometallics* **2001**, *20*, 1255; c) A. Chianese, X. Li, M. Janzen, J. Faller, R. Crabtree, *Organometallics* **2003**, *22*, 1663; d) F. E. Hahn, C. Holtgrewe, T. Pape, M. Martin, E. Sola, L. A. Oro, *Organometallics* **2005**, *24*, 2203; e) M. V. Jiménez, J. Fernández-Tornos, J. J. Pérez-Torrente, F. J. Modrego, S. Winterle, C. Cucnillos, F. J. Lahoz, L. A. Oro, *Organometallics* **2011**, *30*, 5493; f) B. J. Truscott, D. J. Nelson, C. Lujan, A. M. Z. Slawin, S. P. Nolan, *Chem. Eur. J.* **2013**, *19*, 7904; g) K. Riener, M. J. Bitzer, A. Pöthig, A. Raba, M. Cokoja, W. A. Herrmann, F. E. Kühn, *Inorg. Chem.* **2014**, *53*, 12767.
- [9] For recent, excellent reviews on the HA reaction, see: a) T. E. Müller, M. Beller, *Chem. Rev.* **1998**, *98*, 675; b) K. C. Hultzsich, *Adv. Synth. Catal.* **2005**, *347*, 367; c) T. E. Müller, K. C. Hultzsich, M. Yus, F. Foubelo, M. Tada, *Chem. Rev.* **2008**, *108*, 3795; d) A. L. Reznichenko, K. C. Hultzsich, *Top. Organomet. Chem.* **2013**, *43*, 51; e) N. Nishina, Y. Yamamoto, *Top. Organomet. Chem.* **2013**, *43*, 115; f) J. Hannedouche, E. Schulz, *Chem. Eur. J.* **2013**, *19*, 4972; g) L. Huang, M. Arndt, K. Gooßen, H. Heydt, L. J. Gooßen, *Chem. Rev.* **2015**, *115*, 2596; h) E. Bernoud, C. Lepori, M. Mellah, E. Schulz, J. Hannedouche, *Catal. Sci. Technol.* **2015**, *5*, 2017.
- [10] For the most relevant recent literature, see: a) A. Takemiya, J. F. Hartwig, *J. Am. Chem. Soc.* **2006**, *128*, 6042; b) Z. Liu, J. F. Hartwig, *J. Am. Chem. Soc.* **2008**, *130*, 1570; c) K. D. Hesp, M. Stradiotto, *Org. Lett.* **2009**, *11*, 1449; d) C. Metallinos, J. Zaiman, L. Van Belle, L. Dodge, M. Pilkington, *Organometallics* **2009**, *28*, 4534; e) K. D. Hesp, S. Tobisch, M. Stradiotto,

- J. Am. Chem. Soc.* **2010**, *132*, 413; f) X. Shen, S. L. Buchwald, *Angew. Chem. Int. Ed.* **2010**, *49*, 564; *Angew. Chem.* **2010**, *122*, 574; g) L. D. Julian, J. F. Hartwig, *J. Am. Chem. Soc.* **2010**, *132*, 13813; h) Y. Kashiwame, S. Kuwata, T. Ikariya, *Chem. Eur. J.* **2010**, *16*, 766; i) Z. Liu, H. Yamamichi, S. T. Madrahimov, J. F. Hartwig, *J. Am. Chem. Soc.* **2011**, *133*, 2772; j) Y. Kashiwame, S. Kuwata, T. Ikariya, *Organometallics* **2012**, *31*, 8444; k) C. Hua, K. Q. Vuong, M. Bhadbhade, B. A. Messerle, *Organometallics* **2012**, *31*, 1790.
- [11] For first examples of the asymmetric version of this HA reaction with lanthanocenes, published and studied by Marks et al. in detail, see: a) M. R. Gagne, L. Brard, V. Conticello, M. A. Giardello, C. L. Stern, T. J. Marks, *Organometallics* **1992**, *11*, 2003; b) V. P. Conticello, L. Brard, M. A. Giardello, Y. Tsuji, M. Sabat, C. L. Stern, T. J. Marks, *J. Am. Chem. Soc.* **1992**, *114*, 2761; c) M. A. Giardello, V. P. Conticello, L. Brard, M. R. Gagné, T. J. Marks, *J. Am. Chem. Soc.* **1994**, *116*, 10241. For first examples with chiral non-metallocene systems, see: d) S. Hong, S. Tian, M. V. Metz, T. J. Marks, *J. Am. Chem. Soc.* **2003**, *125*, 14768; e) P. N. O'Shaughnessy, P. Scott, *Tetrahedron: Asymmetry* **2003**, *14*, 1979; f) P. N. O'Shaughnessy, P. D. Knight, C. Morton, K. M. Gillespie, P. Scott, *Chem. Commun.* **2003**, 1770; g) D. V. Gribkov, K. C. Hultsch, F. Hampel, *Chem. Eur. J.* **2003**, *9*, 4796; h) J. Collin, J.-C. Daran, E. Schulz, A. Trifonov, *Chem. Commun.* **2003**, 3048.
- [12] For selected examples, see: a) R. Corberán, M. Sanaú, E. Peris, *J. Am. Chem. Soc.* **2006**, *128*, 3974; b) A. Prades, R. Corberán, M. Poyatos, E. Peris, *Chem. Eur. J.* **2008**, *14*, 11474; c) M. J. Cowley, R. W. Adams, K. D. Atkinson, M. C. R. Cockett, S. B. Duckett, G. G. R. Green, J. A. B. Lohman, R. Kerssebaum, D. Kilgour, R. E. Mewis, *J. Am. Chem. Soc.* **2011**, *133*, 6134; d) G. E. Dobreiner, A. Nova, N. D. Schley, N. Hazari, S. J. Miller, O. Eisenstein, R. H. Crabtree, *J. Am. Chem. Soc.* **2011**, *133*, 7547; e) T. Iwai, T. Fujihara, Y. Terao, Y. Tsuji, *J. Am. Chem. Soc.* **2012**, *134*, 1268; f) M. C. Lehman, D. R. Pahls, J. M. Meredith, R. D. Sommer, D. M. Heinekey, T. R. Cundari, E. A. Ison, *J. Am. Chem. Soc.* **2015**, *137*, 3574.
- [13] For examples that feature NHCs within chelate ligands (all of them non-chiral), see: a) E. B. Bauer, G. T. S. Andavan, T. K. Hollis, R. J. Rubio, J. Cho, G. R. Kuchenbeiser, T. R. Helgert, C. S. Letko, F. S. Tham, *Org. Lett.* **2008**, *10*, 1175; b) Z. G. Specht, S. A. Cortes-Llamas, H. N. Tran, C. J. Van Niekerk, C. J. Rancudo, J. A. Golen, C. E. Moore, A. L. Rheingold, T. J. Dwyer, D. B. Grotjahn, *Chem. Eur. J.* **2011**, *17*, 6606; c) R. Zhang, Q. Xu, L. Y. Mei, S. K. Li, M. Shi, *Tetrahedron* **2012**, *68*, 3172. For an example of an Au-catalysed hydroamidation with monodentate NHCs, see: d) H. Li, R. A. Widenhoefer, *Org. Lett.* **2009**, *11*, 2671.
- [14] For asymmetric intermolecular HA reaction with Ir (activated substrates), see: a) R. Dorta, P. Egli, F. Zurcher, A. Togni, *J. Am. Chem. Soc.* **1997**, *119*, 10857; b) J. Zhou, J. F. Hartwig, *J. Am. Chem. Soc.* **2008**, *130*, 12220; c) S. Pan, K. Endo, T. Shibata, *Org. Lett.* **2012**, *14*, 780; d) C. S. Sevov, J. Zhou, J. F. Hartwig, *J. Am. Chem. Soc.* **2012**, *134*, 11960; e) C. S. Sevov, J. Zhou, J. F. Hartwig, *J. Am. Chem. Soc.* **2014**, *136*, 3200.
- [15] R. A. Kelly III, H. Clavier, S. Giudice, N. M. Scott, E. D. Stevens, J. Bordner, I. Samardjiev, C. D. Hoff, L. Cavallo, S. P. Nolan, *Organometallics* **2008**, *27*, 202.
- [16] See the Supporting Information for further details.
- [17] a) C. A. Tolman, *Chem. Rev.* **1977**, *77*, 313. For a recent review on the electronics of NHCs, see: b) D. J. Nelson, S. P. Nolan, *Chem. Soc. Rev.* **2013**, *42*, 6723.
- [18] C. Y. Tang, J. Lednik, D. Vidovic, A. L. Thompson, S. Aldridge, *Chem. Commun.* **2011**, 47, 2523.
- [19] For a review on cyclometalation reactions, see: a) M. Albrecht, *Chem. Rev.* **2010**, *110*, 576. For closely related, selected examples of C–H activation of the NHC wingtips in iridium complexes, see: b) N. M. Scott, R. Dorta, E. D. Stevens, A. Correa, L. Cavallo, S. P. Nolan, *J. Am. Chem. Soc.* **2005**, *127*, 3516; c) C. Y. Tang, A. L. Thompson, S. Aldridge, *J. Am. Chem. Soc.* **2010**, *132*, 10578; d) C. Y. Tang, W. Smith, A. L. Thompson, D. Vidovic, S. Aldridge, *Angew. Chem. Int. Ed.* **2011**, *50*, 1359; *Angew. Chem.* **2011**, *123*, 1395.
- [20] CCDC 1433190 (*syn-2a*), 1433191 (*anti-2a*), 1433192 (*anti-2b*), 1433193 (*anti-3b*), 1433194 (*syn-4a*), 1433195 (*anti-4a*) and 1433196 (*anti-4b*) contain the supplementary crystallographic data for this paper. These data are provided free of charge by The Cambridge Crystallographic Data Centre.
- [21] We are aware of only one example of a fully characterised 14-electron Ir^I species. The complex was obtained through C–H activation/dehydrogenation of a dipp-nacnac ligand, see: W. H. Bernskoetter, E. Lobkovsky, P. J. Chirik, *Organometallics* **2005**, *24*, 6250.
- [22] For a similar iridium complex that incorporates a bulky monophosphine ligand and shows a classical η^2 -coordination of an aryl group, see: A. R. O'Connor, W. Kaminsky, B. C. Chan, D. M. Heinekey, K. I. Goldberg, *Organometallics* **2013**, *32*, 4016.
- [23] For an example that shows a weaker interaction of IMes, see: a) F. Wu, V. K. Dioumaev, D. J. Szalda, J. Hanson, R. M. Bullock, *Organometallics* **2007**, *26*, 5079. For related examples featuring more exotic NHC architectures, see: b) N. Imlinger, K. Wurst, M. R. Buchmeiser, *J. Organomet. Chem.* **2005**, *690*, 4433; c) Y. Zhang, D. Wang, K. Wurst, M. R. Buchmeiser, *J. Organomet. Chem.* **2005**, *690*, 5728; d) E. L. Kolychev, S. Kronig, K. Brandhorst, M. Freytag, P. G. Jones, M. Tamm, *J. Am. Chem. Soc.* **2013**, *135*, 12448.
- [24] Some shifting in the carbene signal when going from neutral to cationic complexes is to be expected, see also: O. Torres, M. Martín, E. Sola, *Organometallics* **2009**, *28*, 863.
- [25] All NMR calculations were performed with the ADF suite at the BP86 level of theory by using a triple- ζ plus two polarisation basis set, see the Supporting Information for further details. A. Liske, K. Verlinden, H. Buhl, K. Schaper, C. Ganter, *Organometallics* **2013**, *32*, 5269.
- [26] a) L. Benhamou, S. Bastin, N. Lugan, G. Lavigne, V. César, *Dalton Trans.* **2014**, 43, 4474; b) V. César, S. Bellemin-Laponnaz, L. H. Gade, *Eur. J. Inorg. Chem.* **2004**, 3436.
- [27] a) S. V. C. Vummaleti, D. J. Nelson, A. Poater, A. Gómez-Suárez, D. B. Cordes, A. M. Z. Slawin, S. P. Nolan, L. Cavallo, *Chem. Sci.* **2015**, *6*, 1895; b) H. Jacobsen, A. Correa, C. Costabile, L. Cavallo, *J. Organomet. Chem.* **2006**, *691*, 4350.
- [28] a) A. J. Arduengo, D. A. Dixon, K. K. Kumashiro, C. Lee, W. P. Power, K. W. Zilm, *J. Am. Chem. Soc.* **1994**, *116*, 6361; b) G. Schreckenbach, T. Ziegler, *J. Phys. Chem.* **1995**, *99*, 606; c) G. Schreckenbach, T. Ziegler, *Int. J. Quantum Chem.* **1997**, *61*, 899.
- [29] a) X. Luan, R. Mariz, C. Robert, M. Gatti, S. Blumentritt, A. Linden, R. Dorta, *Org. Lett.* **2008**, *10*, 5569; b) X. Luan, L. Wu, E. Drinkel, R. Mariz, M. Gatti, R. Dorta, *Org. Lett.* **2010**, *12*, 1912; c) L. Wu, L. Falivene, E. Drinkel, S. Grant, A. Linden, L. Cavallo, R. Dorta, *Angew. Chem. Int. Ed.* **2012**, *51*, 2870; *Angew. Chem.* **2012**, *124*, 2924.
- [30] For catalytic systems providing > 90% ee for at least two pyrrolidine-type products; with rare-earth/Group 4 metals, see: a) D. V. Gribkov, K. C. Hultsch, F. Hampel, *J. Am. Chem. Soc.* **2006**, *128*, 3748; b) M. C. Wood, D. C. Leitch, C. S. Yeung, J. A. Kozak, L. L. Schafer, *Angew. Chem. Int. Ed.* **2007**, *46*, 354; *Angew. Chem.* **2007**, *119*, 358; c) K. Manna, S. Xu, A. D. Sadow, *Angew. Chem. Int. Ed.* **2011**, *50*, 1865; *Angew. Chem.* **2011**, *123*, 1905; d) K. Manna, M. L. Kruse, A. D. Sadow, *ACS Catal.* **2011**, *1*, 1637; e) K. Manna, W. C. Everett, G. Schoendorf, A. Ellern, T. L. Windus, A. D. Sadow, *J. Am. Chem. Soc.* **2013**, *135*, 7235; f) K. Manna, N. Eedugurala, A. D. Sadow, *J. Am. Chem. Soc.* **2015**, *137*, 425; g) X. Zhou, B. Wei, X.-L. Sun, Y. Tang, Z. Xie, *Chem. Commun.* **2015**, 51, 5751. With Mg, see: h) X. Zhang, T. J. Emge, K. C. Hultsch, *Angew. Chem. Int. Ed.* **2012**, *51*, 394; *Angew. Chem.* **2012**, *124*, 406.
- [31] Reference [10f] is the only other report on an enantioselective intramolecular HA reaction of such substrates with a late-transition metal (Rh, between 62 and 91% ee).
- [32] N. Menshutkin, *Z. Phys. Chem. Stoechiom. Verwandtschaftsl.* **1890**, *6*, 41.
- [33] G. O. Nevstad, J. Songstad, *Acta Chem. Scand.* **1984**, *38*, 469.
- [34] For a recent paper that shows similar acceleration/facilitation of this reaction, in this case through incorporation of the tertiary amine into a macrocycle, see: J.-J. Lee, K. J. Stanger, B. C. Noll, C. Gonzalez, M. Marquez, B. D. Smith, *J. Am. Chem. Soc.* **2005**, *127*, 4184.

Received: January 27, 2016
Published online on April 5, 2016